Received: 21 December 2021 | Revised: 3 March 2022 | Accepted: 4 March 2022

DOI: 10.1096/fba.2021-00163

FASEB BioAdvances WILEY

RESEARCH ARTICLE

ToxCast chemical library Wnt screen identifies diethanolamine as an activator of neural progenitor proliferation

Justin M. Wolter[1,2,3] | **Jessica A. Jimenez**[4] | **Jason L. Stein**[1,5] | **Mark J. Zylka**[1,2,3]

[1]UNC Neuroscience Center, The University of North Carolina at Chapel Hill, Chapel Hill, North Carolina, USA

[2]Department of Cell Biology and Physiology, The University of North Carolina at Chapel Hill, Chapel Hill, North Carolina, USA

[3]Carolina Institute for Developmental Disabilities, The University of North Carolina at Chapel Hill, Chapel Hill, North Carolina, USA

[4]Curriculum in Toxicology & Environmental Medicine, The University of North Carolina at Chapel Hill, Chapel Hill, North Carolina, USA

[5]Department of Genetics, The University of North Carolina at Chapel Hill, Chapel Hill, North Carolina, USA

Correspondence
Mark J. Zylka, UNC Neuroscience Center, The University of North Carolina at Chapel Hill, Chapel Hill, NC 27599, USA.
Email: zylka@med.unc.edu

Funding information
M.J.Z. is supported by grants from The Simons Foundation (SFARI, Award ID 393316, 572984, 627144), The National Institute of Environmental Health Sciences (NIEHS; R35ES028366), and The National Institute of Mental Health (NIMH; R01MH120229). J.M.W. was supported by grants from the National Institute for Child Health and Human Development (NICHD; T32HD040127) and a Pfizer-NCBiotech Distinguished Postdoctoral Fellowship in Gene Therapy. J.L.S. was supported by grants from the National Institute of Mental Health (R01MH118349, R00MH102357, and R01MH120125). J.A.J. is supported by the Curriculum in Toxicology and Environmental Medicine Training Grant (NIEHS, T32 ES007126). The UNC Flow Cytometry Core Facility is supported in part by the National Cancer Institute (P30CA016086), awarded to the UNC Lineberger Comprehensive Cancer Center.

Abstract

Numerous autism spectrum disorder (ASD) risk genes are associated with Wnt signaling, suggesting that brain development may be especially sensitive to genetic perturbation of this pathway. Additionally, valproic acid, which modulates Wnt signaling, increases risk for ASD when taken during pregnancy. We previously found that an autism-linked gain-of-function *UBE3A*^{T485A} mutant construct hyperactivated canonical Wnt signaling, providing a genetic means to elevate Wnt signaling above baseline levels. To identify environmental use chemicals that enhance or suppress Wnt signaling, we screened the ToxCast Phase I and II libraries in cells expressing this autism-linked *UBE3A*^{T485A} gain-of-function mutant construct. Using structural comparisons, we identify classes of chemicals that stimulated Wnt signaling, including ethanolamines, as well as chemicals that inhibited Wnt signaling, such as agricultural pesticides, and synthetic hormone analogs. To prioritize chemicals for follow-up, we leveraged predicted human exposure data, and identified diethanolamine (DEA) as a chemical that stimulates Wnt signaling in *UBE3A*^{T485A}–transfected cells, and has a high potential for prenatal exposure in humans. DEA enhanced proliferation in primary human neural progenitor cell lines (phNPC), but did not affect expression of canonical Wnt target genes in NPCs or primary mouse neuron cultures. Instead, we found DEA increased expression of the H3K9 methylation sensitive gene *CALB1*, consistent with competitive inhibition of the methyl donor enzymatic pathways.

Abbreviations: ASD, autism spectrum disorder; BAR, β-catenin-activated reporter; DEA, diethanolamine; FDA, food and drug administration; NPC, neural progenitor cells; phNPC, primary human neural progenitor cells; SMILES, Simplified molecular input line entry system; VPA, valproic acid.

KEYWORDS
diethanolamine, neural progenitor cells, ToxCast, Wnt signaling

1 | INTRODUCTION

Large-scale exome sequencing studies of individuals with autism identified over 100 high-confidence ASD genes.[1–3] Approximately 19% of these ASD genes are associated with the Wnt/β-catenin signaling pathway, suggesting that alterations in Wnt signaling contribute to ASD pathogenesis.[4–9] Members of the Wnt family are secreted signaling proteins that affect the development of nearly every area of the central nervous system.[10] In the developing brain, Wnt establishes the anterior/posterior and dorsoventral axes, and instructs cell fate decisions by regulating the balance between differentiation and proliferation.[11] Constitutive activation of Wnt signaling leads to hyperproliferation of neural progenitor cells and macrocephaly.[12]

Non-genetic environmental factors also contribute to autism risk.[6,13,14] Epidemiological studies link gestational exposure to agricultural pesticides with risk for ASD.[15,16] And, certain environmental use chemicals can mimic transcriptional changes associated with ASD when applied to primary mouse neuron cultures.[17,18] The best characterized environmental risk factor for ASD is valproic acid (VPA), which is prescribed for epilepsy, bipolar depression, and migraine.[19] Prenatal exposure to VPA increases the risk of congenital malformations,[20] ASD,[21,22] and macrocephaly.[23,24] VPA activates Wnt signaling by targeting HDAC1.[25] Furthermore, drugs approved by the FDA for treating behavioral symptoms of ASD (aripipazole, risperidone) can affect Wnt signaling.[26,27] These studies suggest that the developing nervous system may be highly sensitive to chemicals in the environment that modulate Wnt signaling.

Identifying environmental risk factors for neurodevelopmental disorders is a major challenge due to the lack of developmental neurotoxicological data on the vast majority of chemicals.[28] To address this critical need, the Environmental Protection Agency (EPA) created the Tox21 program, which aims to provide platforms and methods to rapidly screen chemicals for potential adverse health effects.[29] Here, we hypothesized that Wnt modulating chemicals will have enhanced effects in cells expressing an ASD-linked gene that, when transiently overexpressed, stimulates Wnt signaling. To test this hypothesis, we screened the EPA ToxCast Phase I and II libraries using a Wnt sensitive luciferase reporter[30] in cells overexpressing UBE3A with an autism-linked T485A mutation (*UBE3A*^{T485A}), a mutation that promotes Wnt signaling.[9,31]

2 | MATERIALS AND METHODS

2.1 | Lentiviral infection of primary mouse cortical neurons

All lentivirus was produced in HEK293T cells using the third-generation packaging plasmids.[32] Supernatant was collected, filtered using 0.45 μM filters, and frozen in single use aliquots. Primary neuron cultures from E15.5 C57Bl/6 mouse embryos were prepared as previously described.[18] Neurons were plated in 96 well plates at 20,000 cells per well. On day three, cells were infected with lentiviruses carrying BAR: luciferase and Tk:*Renilla* in a 5:1 ratio. Cells were incubated for 5 days, then treated with ToxCast chemicals and incubated for 48 h. Cells were lysed and the lysate was used in dual luciferase assays using the Dual-Glo luciferase system (Promega), and measured on the GloMax Discover plate reader (Promega).

2.2 | High-throughput Wnt screen of ToxCast phase I and II libraries

All liquid handling steps of HEK293T ToxCast Phase I/II screen were performed using the Tecan EVO liquid handling robot. These steps included cell plating, chemical library dilution and aliquots, cell dosing, transfections, and luciferase assays. Technical replicates for six control chemicals (three Wnt inhibitors and three Wnt activators) were spiked into random positions in each plate to ensure technical reproducibility and eliminate the risk of plate swaps. HEK293T cells were cultured in DMEM (Gibco) and 10% FBS in the absence of antibiotic in a humid incubator at 37°C with 5% (vol/vol) CO_2. Cells were plated in white opaque 384 well plates at a density of 4500 cells per well. Twenty-four hours post plating cells were transfected with a β-catenin responsive luciferase reporter (BAR),[30] TK-*Renilla*, and pCIG2 *UBE3A*^{T485A} using Fugene 6 (Promega). Cells were treated with chemical libraries four hours post transfection. Cells were lysed 24 h later, and luciferase assays were performed using the Dual-Glo luciferase system (Promega). All steps, including cell culture, treatments, lysis, and luciferase assays were performed in the same plate to minimize technical variation from handling artifacts. Four biological replicates (one well per chemical per

concentration per day) were performed on different days to ensure reproducibility and reduce batch effects.

2.3 | Screen analyses

The "Wnt luciferase ratio" was calculated by dividing the raw firefly value by the raw *Renilla* luciferase value, and median centering within each plate. "Cell Health" was calculated using the raw *Renilla* value median centered within each plate. Biological replicates were averaged, and *p*-values were calculated using a two-tailed *t*-test. To calculate the "Wnt Score" (Wnt activity with a penalty for toxicity) we calculated the mean log2 fold change of the Wnt luciferase ratio for each chemical, calculated the slope of the concentration–response curve for that chemical, and multiplied this by the mean of the Cell Health metric. The EPA spiked in replicate chemicals across plates to assess reproducibility, in addition to the six control chemicals we added. When a chemical was present in multiple plates we averaged the values for each metric.

2.4 | HEK293T versus neuron toxicity comparison

RASL-seq assessed ToxCast Phase I chemical toxicity in primary mouse neuron cultures by spiking in control luciferase RNA in each well, and calculating the ratio of luciferase reads to total number of reads from neurons.[18] We normalized this data by median centering and averaged the values for all concentrations of each chemical. We then compared the measure of cell health from primary neurons to the Cell Health Metric from this screen.

2.5 | Chemical structure clustering

Chemical structure clustering was performed using ChemMineR.[33] SMILES strings were converted to SDF files. Distance matrices were defined using atom-pair properties, and unsupervised hierarchic clustering was performed using R.

2.6 | Estimated human exposure data

Estimated human exposure data were downloaded from Ref [34]. We compared the Wnt Score metric with the 95% confidence interval mg/kg/body weight/day for reproductive age females (defined as 16–49 years old), reasoning that this demographic is most representative of maternal, fetal, and neonatal exposure.

2.7 | DEA in HEK293T cells

DEA was obtained from Sigma-Aldrich (#31589). The panel of luciferase reporter plasmids was a kind gift from the lab of Dr. Ben Major. Luciferase assays were performed as described above. The following day cells were transfected with either pCIG2:empty (eGFP with an IRES carrying empty sequence) or pCIG2 *UBE3A*^{T485A}. Four hours later cells were treated with the indicated concentrations of DEA or vehicle (water) and incubated for 48 h. Cells were lysed and the lysate was used in dual luciferase assays using the Dual-Glo luciferase system (Promega), and measured on the GloMax Discover plate reader (Promega).

2.8 | Primary human neural progenitor cell cultures

Human fetal brain tissue was obtained from the UCLA Gene and Cell Therapy Core following IRB regulations. Primary human (ph)NPCs were grown and differentiated as previously described.[35,36] Briefly, cells were thawed and plated in 10 cm plates with proliferation media (Neurobasal A supplemented with primocin, BIT9500, glutamax, heparin, EGF, FGF, LIF, PDGF) in a humid incubator at 37°C with 5% (vol/vol) CO_2. Cells were mycoplasma tested and confirmed to be mycoplasma free (ATCC, Universal Mycoplasma Detection Kit). For experiments in Figure 1B cells were plated in 96 well plates and infected with lentivirus carrying BAR: luciferase and Tk:*Renilla* in a 5:1 ratio. Cells were incubated for 48 h, then treated with the indicated chemicals. Cells were incubated for an additional 48 h, then lysed and subjected to dual luciferase assays, as described above. For experiments in Figure 5 cells were plated in 96 well plates at a density of 12,500 cells per well. Twenty-four hours later cells were treated with DEA, and incubated for 46 h. We then performed a 2-hour pulse with 10 μM EdU, then fixed the cells with 4% paraformaldehyde. Labelling was performed using the Click-iT EdU fluorescent labeling kit per manufacturer's instructions (Thermo-Fisher Cat. C10337). DNA was labeled using FxCycle Far Red stain (Invitrogen, Cat# F10348). Cells were counted using the Attune NxT. Data were analyzed using the FlowJo software. Recombinant human Wnt-3a (R&D Systems, Cat. 5036-WNP-010) was resuspended in PBS at 1000x concentration.

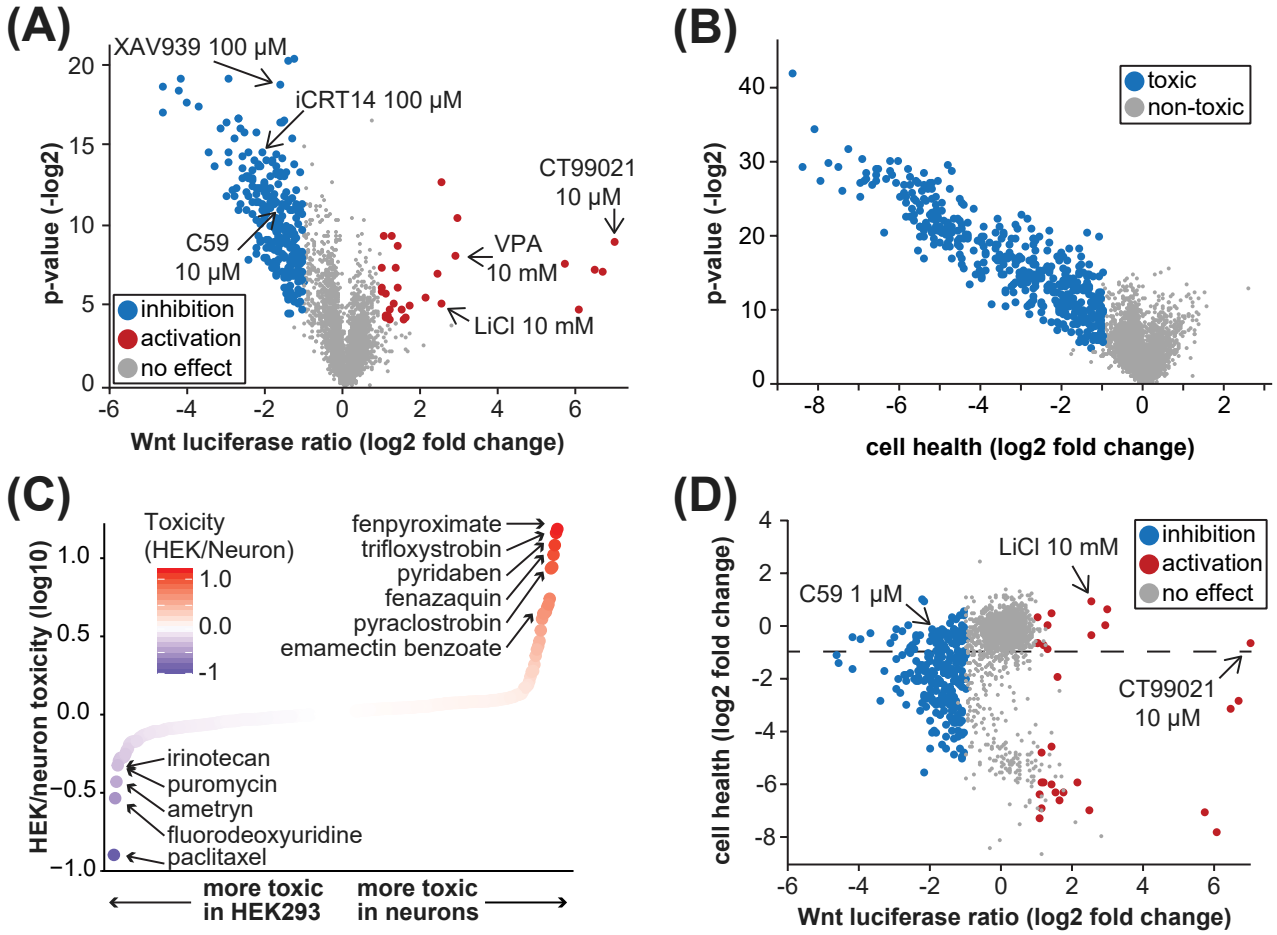

FIGURE 1 Screen to identify ToxCast chemicals that stimulate or inhibit Wnt signaling. (A) ToxCast phase I/II chemicals screened against the Wnt luciferase reporter in HEK293T cells transfected with *UBE3A*^{T485A} expression plasmid. Arrows mark chemicals that were used as positive controls. Each point is a single chemical at a single concentration. P-value represents unpaired *t*-test comparing each chemical with negative control vehicle wells in each plate. (B) Cell health of ToxCast chemicals in HEK293T cells transfected with *UBE3A*^{T485A} expression plasmid. Each point is a single chemical at a single concentration. Decrease in cell health score indicates toxicity. (C) Comparison of ToxCast chemical toxicity in HEK293T cells transfected with *UBE3A*^{T485A} and primary mouse neuron cultures. Toxicity was calculated as the slope of *Renilla* luciferase (internal control) signal across all concentrations of each chemical. (D) Comparison of cell health and Wnt activation measures in HEK293T cells. Each point is a single chemical at a single concentration. Chemicals below the dashed line are those that have toxic effects

2.9 | RNA Extractions and RT-qPCR

RNA extractions were performed using TRIzol (ThermoFisher). cDNA synthesis was performed from 200 ng total RNA using SuperScript IV VILO with ezDNAse (ThermoFisher). qPCR experiments were performed using SsoAdvanced Universal SYBR Green Supermix (NEB) on the Quantstudio5 thermal cycler (Applied Biosystems). Human-specific primers: CALB1 F: ACACAAAATTAGCCGAGTATACAGACC; CALB1 R: CTCAAAAGCCTTATTGAACTCTTTCCC; HES5 F: TGGAGATGGCTGTCAGCTACC; HES5 R: GAGTAGCCTTCGCTGTAGTCC; CCND1 F: TGCA AGGCCTGAACCTGAGG; CCND1 R: TCCATGTTCT GCTGGGCCTGG; AXIN2 F: AATCCGGCCTTCATACA TCGG; AXIN2 R: GGCTCAGAGCTTGACCCTGG; EIF4A2 F: CGGGATTGATGTGCAACAAGTG; EIF4A2 R: ATGGGCATCTCCTCCACTGTAG. Data were normalized to *EIF4A2* using the ΔΔCt method. Two-tailed *t*-tests were used for comparison between vehicle conditions, and two-way ANOVA was used for concentration–response curves.

3 | RESULTS

3.1 | High-throughput screen for environmental use chemicals that modulate Wnt signaling

Given the evidence implicating Wnt signaling in ASD pathogenesis, we set out to test the EPA ToxCast Phase I and Phase II libraries[37] in cells transfected with an ASD-linked

UBE3A^{T485A} mutant expression construct.[31] ToxCast libraries contain chemicals with the potential for human exposure, including pesticides, plasticizers, perfluorinated chemicals, and "failed-pharma" compounds, which were donated by pharmaceutical companies due to toxicity in trials.[37] We were blind to the identities of ToxCast Phase II chemicals during the screen, and were only unblinded after sharing the results of our screen with the EPA.

To quantify Wnt signaling, we used the β-catenin-activated reporter (BAR) luciferase reporter, which contains 12 tandem binding sites for the TCF/LEF transcription factor.[30] We co-transfected a *Renilla* luciferase reporter driven by the thymidine kinase (TK) promoter as an internal control to assess cell viability and toxicity. Overexpression of *UBE3A*^{T485A} activates the Wnt reporter by inhibiting proteasome-dependent degradation of β-catenin.[9] To identify a representative cellular context in which to perform the screen, we tested known Wnt activators in primary mouse cortical neurons, phNPCs, and HEK293T cells (Figures S1-S3A–C). Control chemicals included VPA,[25] the GSK3β inhibitor CT99021,[38] and lithium chloride.[39] We found context-specific effects, with LiCl not activating the Wnt reporter in primary mouse neurons (Figure S1-S3A), and VPA not activating the Wnt reporter in phNPCs (Figure S1-S3B). HEK293T were the only cells that demonstrated Wnt activation of all three chemicals, therefore we chose these cells to perform the screen (Figure S1-S3C). Wnt inhibitors and activators received a positive Z-factor, a statistical measure of assay suitability for high-throughput screening[40] (Figure S1-S3D).

Our two endpoints were Wnt luciferase ratio (BAR/*Renilla*, Figure 1A) and "cell health" (*Renilla* values, Figure 1B) (see Materials and Methods). We considered putative Wnt modulators as those with abs (log2 fold change) > 1 compared to vehicle, and p-value < 0.05 (Figure 1A, Table S1). All control chemicals performed as expected (arrows, Figure 1A).

3.2 | Toxicity of ToxCast phase I/II chemicals

Many of the ToxCast chemicals exhibited concentration-dependent toxicity (log2 fold change < −1, and p-value < 0.05, Table S1, Figure 1B). Previously, we tested the ToxCast Phase I library, which contains mostly pesticides,[37] in primary mouse neuron cultures using RNA-seq as well as RASL-seq—a massively pooled transcriptomic assay.[17,18] In the RASL-seq experiments we also estimated neuronal toxicity by comparing total read counts per well to a luciferase mRNA spike in control. To identify chemicals with context- specific toxicity, we compared the toxicity values in HEK293T cells (Figure 1B) with those in primary mouse neurons (Figure 1C). The chemicals which were specifically toxic in HEK293T cells were mechanistically broad (Table S2), but typically exert antimitotic effects, such as the chemotherapeutics paclitaxel, fluorodeoxyuridine, and irinotecan.[41,42] Among these chemicals were also environmental use pesticides such as ametryn, the most widely used herbicide in sugarcane production and a frequent contaminant in aquatic environments.[43,44] In contrast to the broad mechanisms of toxicity in HEK293T cells, the chemicals that were most toxic to neurons were mitochondrial complex I and III inhibitors. These included fenpyroximate, trifloxystrobin, pyridaben, fenazaquin, and pyraclostrobin (Figure 1C, Table S2).[45,46] This class of chemicals is functionally related to rotenone (Table S2), which is implicated in Parkinson's disease.[47,48] Emamectin benzoate, a chemical that binds with high affinity to invertebrate GABA receptors,[49,50] was also selectively toxic in mouse neurons.

We next compared Wnt modulation with toxicity, and found that many chemicals that activated or inhibited the Wnt reporter were also toxic (Figure 1D). This is in contrast to our control chemicals which modulated Wnt without strong toxicity (Figure 1D, Figure 2A,B). Therefore, we generated a metric termed the "Wnt Score," which reflects the potency of each drug across multiple concentrations with a penalty for toxicity (See Materials and Methods, Figure S2). All the control chemicals segregated to the top of this list (Figure 2A). To identify high-confidence non-toxic Wnt modulators, we filtered for those with $p < 0.05$, abs (log2 fold change) > 1, and Wnt score > 0.4.

3.3 | Structural and functional comparisons of nontoxic Wnt modulators

Structural comparisons of chemical libraries can be used to group chemicals with similar structures to infer common functions and molecular targets. To characterize structural similarities in the ToxCast chemicals, we used SMILES strings to perform hierarchical clustering and multidimensional scaling.[33] The most potent Wnt activator in the ToxCast library was pharmaGSID_48505, which has structural similarity with CT99021 (Figure 2B, Figure S3A,B). The similarity in effect size and structure between these two molecules suggests pharmaGSID_48505 targets GSK3β, but the enhanced toxicity suggests it is not as specific as CT99021 (Figures 3A,B). The next cluster of Wnt activators contains several forms of ethanolamine (Figure 2B,C). Ethanolamines are bifunctional chemicals, containing a primary amine group and a primary ethanol group. Ethanolamine forms the head group of the phospholipid phosphatidylethanolamine, which is highly abundant in the inner leaflet of cell membranes,[51] and comprises ~45% of all phospholipids in the brain.[52] Both ethanolamine and

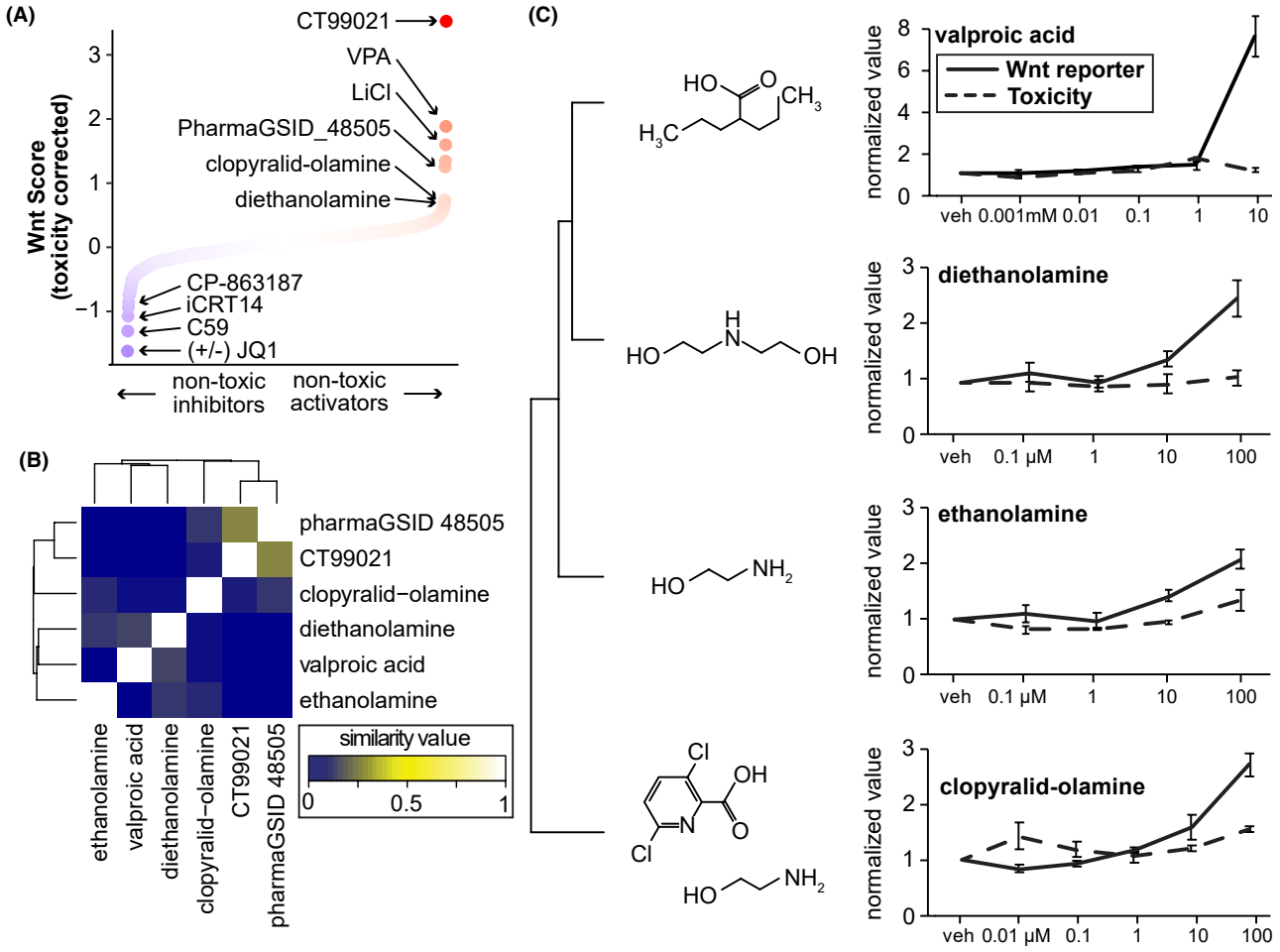

FIGURE 2 Nontoxic Wnt activators in HEK293T cells. (A) Toxicity corrected Wnt luciferase ratio (Wnt Score), which combines all concentrations of each chemical and imparts a penalty for toxicity (mean luciferase ratio of all concentrations (log2 fold change), multiplied by the mean *Renilla* values for all concentrations). Positive control chemicals for both activation and inhibition rose to the top of this list. (B) Comparison of chemical structures of nontoxic Wnt activators using SMILES strings and hierarchical clustering. (C) Concentration–response curves for Wnt luciferase signal and toxicity scores for the ethanolamine cluster. Values normalized to vehicle

diethanolamine (DEA) activated the Wnt reporter without toxic effects (Figure 2C), while triethanolamine had no effect (Figure S3C). DEA has marginal structural similarity to VPA (Figure 2B). Clopyralid-olamine, a mixture of clopyralid and ethanolamine, also activated the Wnt reporter (Figure 2C). However, clopyralid alone had no effect (Figure S3D), suggesting that ethanolamine in this mixture was responsible for activating the Wnt reporter.

Wnt inhibitors were substantially more numerous than activators, highlighting the benefit of screening the Wnt reporter in cells transfected with *UBE3A*^{T485A}, which activates Wnt signaling (Figure 3A). Multiple agricultural pesticides inhibited the Wnt reporter, and these were structurally diverse (Figure 3A). These included the mitochondria complex I inhibitor tebufenpyrad (Figure 3B), and flufenacet, which inhibits synthesis of very long chain fatty acids (Figure 3C).[53,54] Three inhibitors of p38 were also identified (Figure 3A), including CP-863187 which is a highly potent and selective p38 inhibitor (Figure 3D).[55] P38 regulates the canonical Wnt pathway through GSK3β,[56] again highlighting GSK3β as a central regulatory node of the Wnt pathway. Four clusters resolved when comparing chemical similarity, including synthetic estrogens (Figure 3E), thyroid hormone analogs (Figure 3F), glucocorticoid and steroid hormones (Figure 3G), and agricultural fungicides (Figure 3H). The crosstalk between these hormone signaling pathways and Wnt signaling is well established.[57–61] These results raise the possibility that exposure to multiple chemicals with structural and functional similarity might have additive effects by acting through the same molecular pathways.

3.4 | Prioritizing chemicals using predicted human exposure data

Humans are exposed to thousands of environmental use chemicals, yet exposure data are not available for the

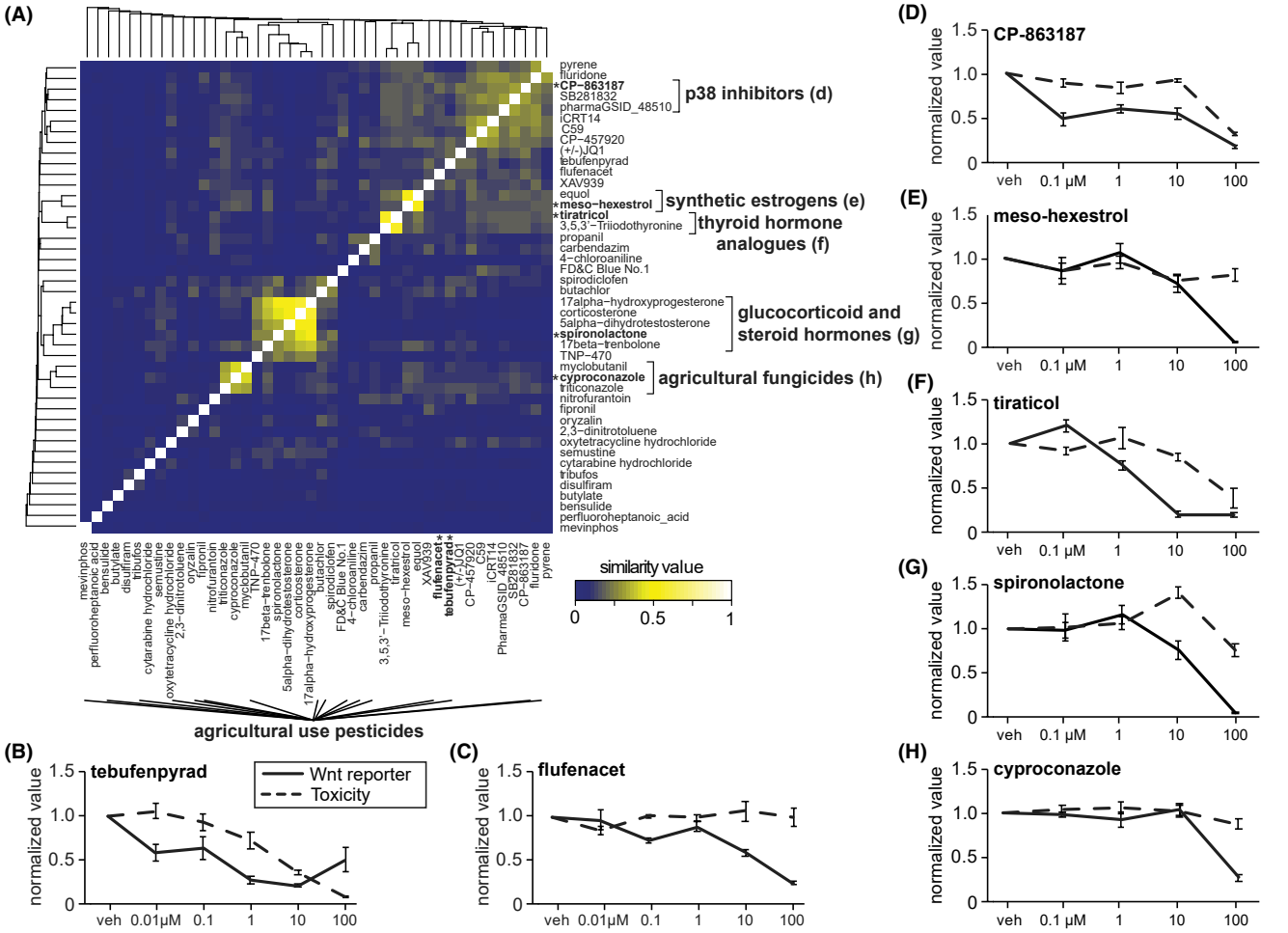

FIGURE 3 Nontoxic Wnt inhibitors in HEK293T cells. (A) Comparison of chemical structures of nontoxic Wnt inhibitors using SMILE strings and hierarchical clustering. Representative chemicals displayed in B–H marked by asterisks. (B–H) Concentration–response curves for Wnt luciferase signal and toxicity scores for representative chemicals of each class

majority of these chemicals.[62] Instead, exposure estimates can be generated using various parameters, including urine biomonitoring of representative chemicals, chemical use classes, and production volume.[34] We used these estimates to prioritize chemicals for more detailed validation experiments (Figure 4). We focused on exposure (mg/kg/body weight/day) predictions for reproductive females (age 16–49), reasoning that this age group best represents in utero exposure estimates (Figure 4, Table S3). The inhibitor with the highest relative exposure predictions was FD&C Blue No.1 (Figure 4). This dye has been approved for use in foods since the early 1900's, and is considered safe and non-toxic by the FDA. It is deep blue in color, which visibly altered the color of cell media, which could interfere with the sensitivity of the luciferase assay. For these reasons we did not pursue this chemical for further experimental validation.

The next Wnt modulator with high exposure predictions was DEA, which was in the 98th percentile of predicted exposure volume for all ~8000 chemicals in the Tox21 set (Figure 4).[34] DEA is used in a wide range of products, including adhesives, printing inks, paint, pigments, and paper, among others.[63] DEA is capable of absorbing through the skin, therefore the most likely route of human exposure is dermally through liquid laundry and dish detergents, shampoos, and soaps,[63,64] where it functions as a surfactant and pH adjuster.[65] It is also used in manufacturing, where it is estimated that ~800,000 workers are exposed to DEA through occupations such as metalwork and road paving.[63] There is inadequate epidemiological data for DEA exposure in humans, but DEA is classified as possibly carcinogenic in humans based on animal models,[66] where dermal exposure demonstrates carcinogenic activity.[67] DEA accumulates in specific tissues following repeat exposure, including the brain, where it is incorporated into phospholipids.[68] DEA has also been shown to influence hippocampal neural progenitor proliferation at high doses in vitro[69] and in vivo.[70,71]

DEA is structurally similar to endogenous ethanolamine and choline. Cells and animals treated with DEA

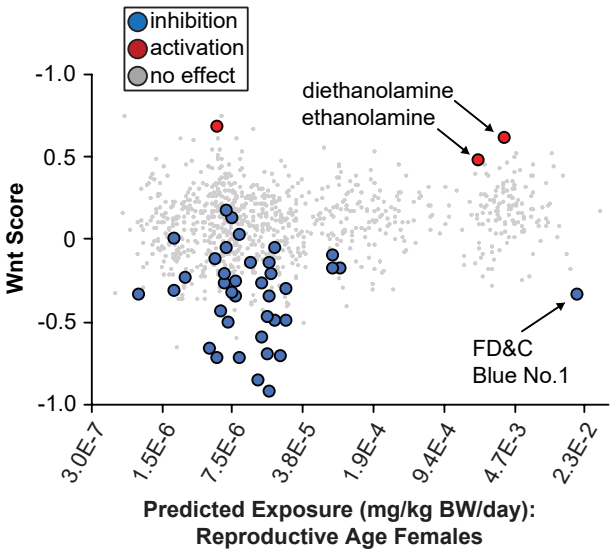

FIGURE 4 Human exposure prediction data for ToxCast chemicals. Predicted exposure of reproductive age females to ToxCast chemical libraries. Chemicals with nontoxic Wnt modulation from Figures 2,3 are colored

phenocopy choline deficiency, likely via competitive inhibition of choline metabolism.[69,72] However, there are no previous reports linking DEA to Wnt signaling, nor to any other developmental signaling pathways. For these reasons we decided to focus on DEA in follow-up experiments. Using commercially obtained DEA, we tested the specificity of DEA in HEK293T cells against luciferase reporters that are sensitive to various signaling pathways. DEA concentration-dependently activated the Wnt reporter, with slight but statistically significant activation of the TGFβ reporter (Figure 5A). Wnt and TGFβ share many downstream target genes, and components of the two pathways are known to interact.[73] We treated primary neuron cultures from wild-type mice with DEA, but did not observe activation of the Wnt luciferase reporter (Figure 5B), suggesting that DEA may have context-specific effects similar to other Wnt agonists (Figure S1-S3A–C). DEA increased the expression of the constitutively active *Renilla* luciferase reporter at low doses, suggesting that DEA may have a positive effect on neuronal viability and/or transcriptional output in cultures (Figure 5B).

We next tested whether genetic background influenced the activity of DEA. We transfected HEK293T cells with either an empty plasmid, or one containing the autism-linked $UBE3A^{T485A}$ mutant construct, and tested the effect of DEA on the Wnt reporter over a wide range of concentrations. Notably, DEA activated the Wnt reporter at 100-fold lower concentrations when transfected with $UBE3A^{T485A}$ (Figure 5C). DEA has previously been shown to decrease proliferation and increase apoptosis of mouse NPCs in vitro and in vivo.[69,70] In vivo, DEA affects hippocampal NPC proliferation at 80 mg/kg,[70] which is substantially higher than what is predicted for human exposure (~0.0038 mg/kg bodyweight per day). Therefore, we sought to determine the lowest concentration at which DEA alters NPC proliferation using two genetically distinct phNPC lines.[35] We compared DEA to known chemical Wnt modulators, including the Wnt activators CT99021, and lithium chloride. Each of the control chemicals increased proliferation as expected (Figure 5D,E). DEA increased proliferation in a concentration-dependent fashion; the magnitude was similar to that of lithium chloride (Figure 5D,E). DEA was active at the lowest concentration tested (50 μM) in one cell line. We observed that higher concentrations were noticeably toxic to phNPCs (Figure 5E).

We next tested whether DEA affected the expression of target genes of the canonical Wnt signaling pathway in phNPCs. DEA did not affect the expression of known canonical Wnt target genes (Figure 5F–H). Adding Wnt3a protein to culture media affected Wnt target genes as expected, but DEA did not further increase expression of these genes. So how is it that DEA is affecting proliferation (Figure 5C,D), viability (Figure 5B), and an exogenous Wnt reporter (Figure 5A), seemingly independent of endogenous Wnt signaling? Previous studies found that DEA negatively affects choline uptake and processing pathways by competitive inhibition of choline processing proteins.[69] Choline deficiency is especially crucial in brain development,[74] where deficiency reduces expression of genes controlling the cell cycle, and causes hypomethylation of CpG sites and the H3K9me1/2 histone modifications.[75,76] A previous study found that choline deficiency in primary mouse NPC cultures affects both DNA and H3K9 methylation in an RE1 site in the promoter of the *CALB1* gene, leading to increased *CALB1* expression.[75] Therefore, we tested whether DEA could affect *CALB1* expression in phNPC cultures. We found that DEA increased expression of *CALB1* in both the presence and absence of Wnt stimulation, and at low doses which also activate NPC proliferation (Figure 5I). We further validated these findings in a panel of 12 genetically distinct phNPC lines, and found that the majority of lines increased *CALB1* expression in response to DEA (Figure 5J). In all, this data suggest that DEA may be affecting gene expression in a manner consistent with altered methylation patterns and choline deficiency.

4 | DISCUSSION

Here, we screened a library of environmental use chemicals for their ability to modulate a Wnt sensitive reporter in cells overexpressing $UBE3A^{T485A}$, an

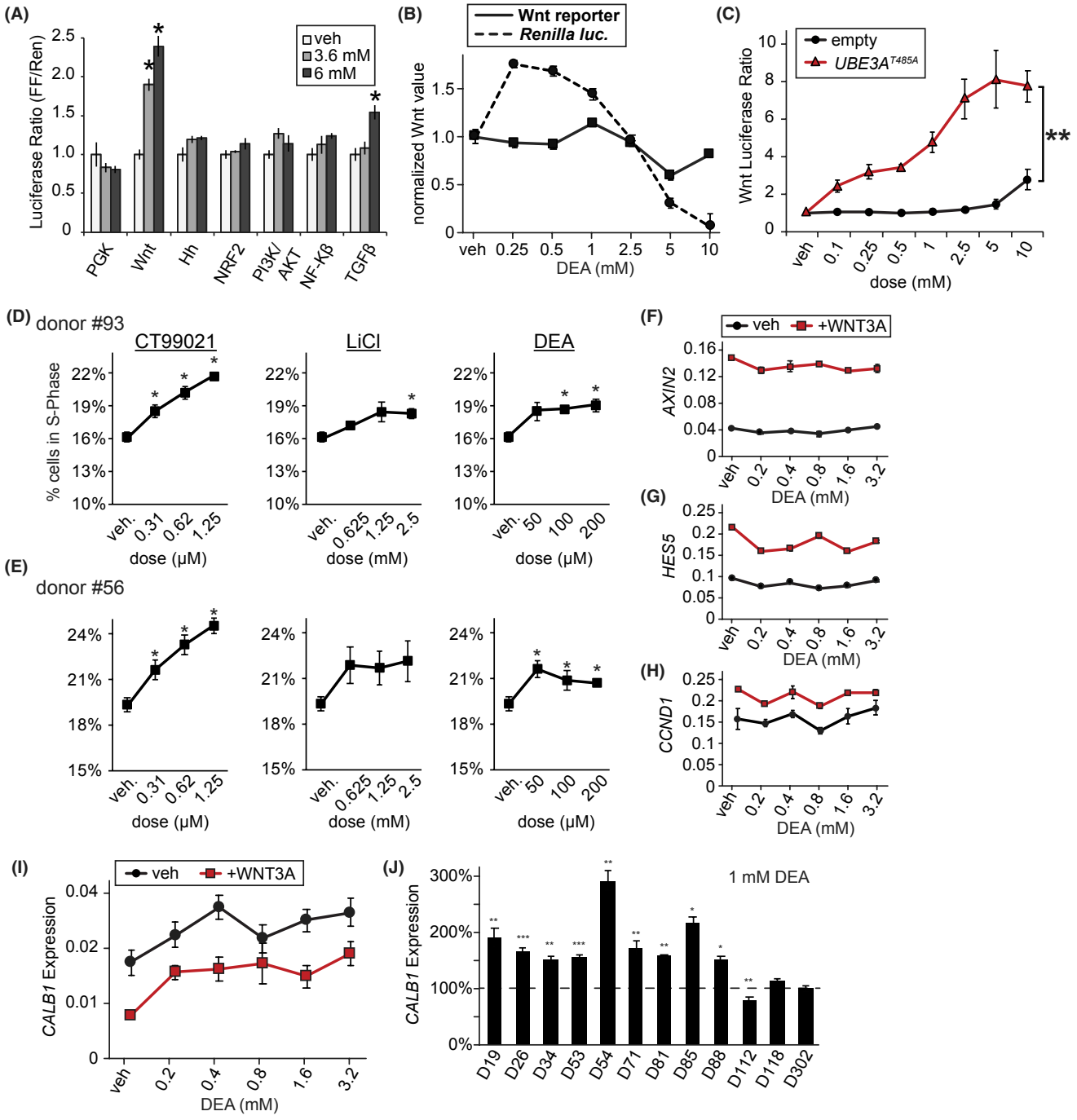

FIGURE 5 DEA activates Wnt signaling and proliferation. (A) The effect of DEA in HEK293T cells on several luciferase reporters that measure developmental signaling pathways. Experiments done in the absence of *UBE3A*^{T485A} overexpression. Tk:Renilla co-transfected for internal control. PGK (ubiquitous promoter, negative control), Hh (Hedgehog). Data normalized to vehicle for each reporter. *T*-test, $^{*}p < 0.05$, $n = 4$. (B) E15.5 primary neuron cultures from C57Bl/6 mice were infected with lentivirus carrying the BAR Wnt firefly luciferase reporter, and a constitutively active *Renilla* luciferase reporter on DIV3. On DIV5 cells were treated with the indicated doses of DEA, and lysate was subjected to dual luciferase assay on DIV7. Wnt reporter was normalized to *Renilla* luciferase signal. $n = 4$. (C) Concentration–response curve of DEA in HEK293T cells on Wnt luciferase reporter in the presence of either empty plasmid, or *UBE3A*^{T485A} overexpression. ANOVA, effect of genotype on Wnt response, $^{**}p < 0.01$. (D,E) Proliferation rates of Wnt control chemicals and DEA in two primary human neural progenitor cell lines. Cells treated for 46 h with indicated chemical and concentration, followed by a 2 h pulse with EdU. Cells analyzed by flow cytometry. *T*-test, $^{*}p < 0.05$, $n = 4$. (F–H) A phNPC line was treated with the indicated doses of DEA with and without 200 ug/mL recombinant human Wnt3a protein, followed by a 2 day incubation and RT-qPCR for the indicated genes. Gene expression was normalized to the gene *EIF4A2*. $n = 4$. (I) A phNPC line was treated with the indicated doses of DEA with and without 200 ug/ml recombinant human Wnt3a protein, followed by a 2 day incubation and RT-qPCR for the indicated genes. Gene expression was normalized to the gene *EIF4A2*. $n = 4$. (J) A panel of 12 additional phNPC lines were treated with vehicle or 1 mM DEA, followed by RT-qPCR for *CALB1*. Expression was normalized to *EIF4A2*, and vehicle-treated cells (dashed line). $^{*}p < 0.05$, $^{**}p < 0.01$, $^{***}p < 0.001$. $n = 4$

autism-linked gene that stimulates Wnt signaling at baseline. Previously, the EPA tested the ToxCast libraries for Wnt activation using a similar TCF7 reporter construct.[77] Our approach is different for two reasons. First, in HEK293T cells TCF/LEF reporters are largely not expressed above baseline levels without additional treatment, which prevents detection of Wnt inhibitors. Second, we evaluated Wnt signaling in a genetically "sensitized" background, which we hypothesized would enhance the effects of Wnt modulators.

By comparing chemical structures, we identified classes of chemicals with shared effects on Wnt signaling, including synthetic estrogens, thyroid hormones, glucocorticoid and steroid hormones, and agricultural fungicides. Aside from PharmaGSID_48505, the primary cluster of nontoxic Wnt activators were ethanolamines, which are predicted to have relatively high levels of exposure in reproductive age females and children age 6–11 (Figure 4). We found that DEA activated the Wnt signaling reporter in baseline conditions in HEK293T cells, but overexpressing the autism-linked *UBE3A*^{T485A} mutation amplified DEA's effect on Wnt signaling (Figure 5). Consistent with the role on Wnt in regulating proliferation, we observed an increase in proliferation in phNPCs. However, follow-up experiments failed to show that DEA has direct effects on canonical Wnt target genes in phNPCs or primary neurons. Instead, we found that low concentrations of DEA altered expression of the methylation sensitive gene *CALB1*. The expression of many components of the Wnt pathway is regulated by DNA and histone methylation, and altered promoter methylation of genes implicated in Wnt signaling is observed in a variety of tumor types.[78] Choline is a precursor to S-adenosyl methionine, which is a substrate for DNA and histone methyltransferases.[79] DEA affects methylation patterns via competitive inhibition of the methyl donor enzymatic pathway due to its structural similarity to choline.[80] We hypothesize that the combination of DEA and *UBE3A*^{T485A} overexpression may substantially alter both the transcriptional and posttranslational landscape, resulting in indirect activation of the Wnt luciferase reporter. Determining whether DEA alters DNA and histone methylation in vivo, and whether additive effects exist in different contexts will clarify the relevance of our findings.

In animal models, DEA exposure has effects on several tissue/organ systems. Mice treated with DEA for 2 years develop higher rates of kidney and liver tumors (data reviewed in[64]). These tumors had high rates of mutations in exon two of the β-catenin gene, and demonstrated abnormal nuclear localization of β-catenin, indicative of constitutively active Wnt signaling.[81] Topical treatment of DEA on pregnant mice reduces embryonic viability, and reduces proliferation of embryonic hippocampal neural progenitors in vivo.[70] At high doses, DEA was found to reduce proliferation of cultured murine NPCs via inhibition of choline uptake.[69] Choline is an essential nutrient crucial for normal brain development,[74] and DEA affects methylation patterns that mimic choline deficiency.[80]

The use of DEA in cosmetics was banned in Europe and Canada following concerns about DEA as a carcinogen.[82,83] The FDA and the National Toxicology Program have likewise found an association between DEA and cancer in lab animals, and provide information on the use of DEA and its derivatives in cosmetics (https://www.fda.gov/cosmetics/cosmetic-ingredients/diethanolamine). However, as of this writing, DEA is approved in the United States as long as it does not comprise >5% of the total product composition.[64] To our knowledge there have been no epidemiological studies suggesting a role, or lack thereof, of DEA in increasing risk for neurodevelopmental disorders. Our data suggest that genetic background (i.e., *UBE3A*^{T485A} expression) may enhance the effects of DEA. Given these findings and the predicted high level of exposure in humans, including women of childbearing age, additional studies are warranted, particularly with regard to exposure and neurodevelopmental outcomes in genetically sensitized backgrounds.

ACKNOWLEDGMENTS

The authors thank Tammy Havener and the UNC Catalyst for Rare diseases for use of the high-throughput screening facility, Thomas Girke for technical assistance, John Wambaugh for providing human exposure prediction data, Keith Houck at the EPA for providing the ToxCast libraries, and Steven Zeisel for his helpful comments.

AUTHOR CONTRIBUTIONS

JMW and MJZ designed the experiments and wrote the manuscript. JMW performed all experiments and analysis. JJ performed the experiments in Figure 5A. JLS provided reagents and protocols for performing human neural progenitor cultures.

REFERENCES

1. Satterstrom, F. K., Kosmicki, J. A., Wang, J., et al. (2020) Large-scale exome Sequencing study implicates both developmental and functional changes in the neurobiology of Autism. *Cell* 180, 568–584 e523, 568, 584.e23
2. Feliciano P, Zhou X, Astrovskaya I, et al. Exome sequencing of 457 autism families recruited online provides evidence for autism risk genes. *NPJ Genom Med*. 2019;4:19.
3. Martin PM, Yang X, Robin N, et al. A rare WNT1 missense variant overrepresented in ASD leads to increased WNT signal pathway activation. *Transl Psychiatry*. 2013;3:e301.

4. Packer A. Enrichment of factors regulating canonical Wnt signaling among autism risk genes. *Mol Psychiatry*. 2018;23:492-493.
5. Pinto D, Delaby E, Merico D, et al. Convergence of genes and cellular pathways dysregulated in autism spectrum disorders. *Am J Hum Genet*. 2014;94:677-694.
6. de la Torre-Ubieta L, Won H, Stein JL, Geschwind DH. Advancing the understanding of autism disease mechanisms through genetics. *Nat Med*. 2016;22:345-361.
7. Kwan V, Unda BK, Singh KK. Wnt signaling networks in autism spectrum disorder and intellectual disability. *J Neurodev Disord*. 2016;8:45.
8. Marchetto MC, Belinson H, Tian Y, et al. Altered proliferation and networks in neural cells derived from idiopathic autistic individuals. *Mol Psychiatry*. 2017;22:820-835.
9. Yi JJ, Paranjape SR, Walker MP, et al. The autism-linked UBE3A T485A mutant E3 ubiquitin ligase activates the Wnt/beta-catenin pathway by inhibiting the proteasome. *J Biol Chem*. 2017;292:12503-12515.
10. Mulligan KA, Cheyette BN. Wnt signaling in vertebrate neural development and function. *J Neuroimmune Pharmacol*. 2012;7:774-787.
11. Noelanders R, Vleminckx K. How Wnt signaling builds the brain: bridging development and disease. *Neuroscientist*. 2017;23:314-329.
12. Chenn A, Walsh CA. Regulation of cerebral cortical size by control of cell cycle exit in neural precursors. *Science*. 2002;297:365-369.
13. Gaugler T, Klei L, Sanders SJ, et al. Most genetic risk for autism resides with common variation. *Nat Genet*. 2014;46:881-885.
14. Modabbernia A, Velthorst E, Reichenberg A. Environmental risk factors for autism: an evidence-based review of systematic reviews and meta-analyses. *Mol Autism*. 2017;8:13.
15. Shelton JF, Geraghty EM, Tancredi DJ, et al. Neurodevelopmental disorders and prenatal residential proximity to agricultural pesticides: the CHARGE study. *Environ Health Perspect*. 2014;122:1103-1109.
16. Roberts EM, English PB, Grether JK, Windham GC, Somberg L, Wolff C. Maternal residence near agricultural pesticide applications and autism spectrum disorders among children in the California Central Valley. *Environ Health Perspect*. 2007;115:1482-1489.
17. Pearson BL, Simon JM, McCoy ES, Salazar G, Fragola G, Zylka MJ. Identification of chemicals that mimic transcriptional changes associated with autism, brain aging and neurodegeneration. *Nat Commun*. 2016;7:11173.
18. Simon JM, Paranjape SR, Wolter JM, Salazar G, Zylka MJ. High-throughput screening and classification of chemicals and their effects on neuronal gene expression using RASL-seq. *Sci Rep*. 2019;9:4529.
19. Thomas RH. Valproate: life-saving, life-changing. *Clin Med (Lond)*. 2018;18:s1-s8.
20. Meador K, Reynolds MW, Crean S, Fahrbach K, Probst C. Pregnancy outcomes in women with epilepsy: a systematic review and meta-analysis of published pregnancy registries and cohorts. *Epilepsy Res*. 2008;81:1-13.
21. Williams G, King J, Cunningham M, Stephan M, Kerr B, Hersh JH. Fetal valproate syndrome and autism: additional evidence of an association. *Dev Med Child Neurol*. 2001;43:202-206.
22. Christensen J, Gronborg TK, Sorensen MJ, et al. Prenatal valproate exposure and risk of autism spectrum disorders and childhood autism. *Jama*. 2013;309:1696-1703.
23. Go HS, Kim KC, Choi CS, et al. Prenatal exposure to valproic acid increases the neural progenitor cell pool and induces macrocephaly in rat brain via a mechanism involving the GSK-3beta/beta-catenin pathway. *Neuropharmacol*. 2012;63:1028-1041.
24. Sabers A, Bertelsen FC, Scheel-Kruger J, Nyengaard JR, Moller A. Long-term valproic acid exposure increases the number of neocortical neurons in the developing rat brain. A possible new animal model of autism. *Neurosci Lett*. 2014;580:12-16.
25. Phiel CJ, Zhang F, Huang EY, Guenther MG, Lazar MA, Klein PS. Histone deacetylase is a direct target of valproic acid, a potent anticonvulsant, mood stabilizer, and teratogen. *J Biol Chem*. 2001;276:36734-36741.
26. Alimohamad H, Sutton L, Mouyal J, Rajakumar N, Rushlow WJ. The effects of antipsychotics on beta-catenin, glycogen synthase kinase-3 and dishevelled in the ventral midbrain of rats. *J Neurochem*. 2005;95:513-525.
27. Pan B, Huang XF, Deng C. Chronic administration of aripiprazole activates GSK3beta-dependent signalling pathways, and up-regulates GABAA receptor expression and CREB1 activity in rats. *Sci Rep*. 2016;6:30040.
28. Dix DJ, Houck KA, Martin MT, Richard AM, Setzer RW, Kavlock RJ. The ToxCast program for prioritizing toxicity testing of environmental chemicals. *Toxicol Sci*. 2007;95:5-12.
29. Thomas RS, Paules RS, Simeonov A, et al. The US federal Tox21 program: a strategic and operational plan for continued leadership. *ALTEX*. 2018;35:163-168.
30. Major MB, Camp ND, Berndt JD, et al. Wilms tumor suppressor WTX negatively regulates WNT/beta-catenin signaling. *Science*. 2007;316:1043-1046.
31. Yi JJ, Berrios J, Newbern JM, et al. An Autism-linked mutation disables phosphorylation control of UBE3A. *Cell*. 2015;162:795-807.
32. Dull T, Zufferey R, Kelly M, et al. A third-generation lentivirus vector with a conditional packaging system. *J Virol*. 1998;72:8463-8471.
33. Backman TW, Cao Y, Girke T. ChemMine tools: an online service for analyzing and clustering small molecules. *Nucleic Acids Res*. 2011;39:W486-W491.
34. Wambaugh JF, Wang A, Dionisio KL, et al. High throughput heuristics for prioritizing human exposure to environmental chemicals. *Environ Sci Technol*. 2014;48:12760-12767.
35. Stein JL, de la Torre-Ubieta L, Tian Y, et al. A quantitative framework to evaluate modeling of cortical development by neural stem cells. *Neuron*. 2014;83:69-86.
36. Wolter JM, Mao H, Fragola G, et al. Cas9 gene therapy for Angelman syndrome traps Ube3a-ATS long non-coding RNA. *Nature*. 2020;587:281-284.
37. Richard AM, Judson RS, Houck KA, et al. ToxCast chemical landscape: paving the road to 21st century Toxicology. *Chem Res Toxicol*. 2016;29:1225-1251.
38. Cohen P, Goedert M. GSK3 inhibitors: development and therapeutic potential. *Nat Rev Drug Discov*. 2004;3:479-487.
39. Klein PS, Melton DA. A molecular mechanism for the effect of lithium on development. *Proc Natl Acad Sci U S A*. 1996;93:8455-8459.

40. Zhang JH, Chung TD, Oldenburg KR. A simple statistical parameter for use in evaluation and validation of high throughput screening assays. *J Biomol Screen*. 1999;4:67-73.
41. Stathopoulos GP, Dimitroulis J, Antoniou D, et al. Front-line paclitaxel and irinotecan combination chemotherapy in advanced non-small-cell lung cancer: a phase I-II trial. *Br J Cancer*. 2005;93:1106-1111.
42. Allen-Mersh TG, Earlam S, Fordy C, Abrams K, Houghton J. Quality of life and survival with continuous hepatic-artery floxuridine infusion for colorectal liver metastases. *Lancet*. 1994;344:1255-1260.
43. Lin HD, Hsu LS, Chien CC, Chen SC. Proteomic analysis of ametryn toxicity in zebrafish embryos. *Environ Toxicol*. 2018;33:579-586.
44. Santos T, Cancian G, Neodini DN, et al. Toxicological evaluation of ametryn effects in Wistar rats. *Exp Toxicol Pathol*. 2015;67:525-532.
45. Charli A, Jin H, Anantharam V, Kanthasamy A, Kanthasamy AG. Alterations in mitochondrial dynamics induced by tebufenpyrad and pyridaben in a dopaminergic neuronal cell culture model. *Neurotoxicol*. 2016;53:302-313.
46. van der Stel W, Carta G, Eakins J, et al. Multiparametric assessment of mitochondrial respiratory inhibition in HepG2 and RPTEC/TERT1 cells using a panel of mitochondrial targeting agrochemicals. *Arch Toxicol*. 2020;94:2707-2729.
47. Priyadarshi A, Khuder SA, Schaub EA, Shrivastava S. A meta-analysis of Parkinson's disease and exposure to pesticides. *Neurotoxicol*. 2000;21:435-440.
48. Sherer TB, Richardson JR, Testa CM, et al. Mechanism of toxicity of pesticides acting at complex I: relevance to environmental etiologies of Parkinson's disease. *J Neurochem*. 2007;100:1469-1479.
49. Xu X, Sepich C, Lukas RJ, Zhu G, Chang Y. Emamectin is a non-selective allosteric activator of nicotinic acetylcholine receptors and GABAA/C receptors. *Biochem Biophys Res Commun*. 2016;473:795-800.
50. Yen TH, Lin JL. Acute poisoning with emamectin benzoate. *J Toxicol Clin Toxicol*. 2004;42:657-661.
51. Bakovic M, Fullerton MD, Michel V. Metabolic and molecular aspects of ethanolamine phospholipid biosynthesis: the role of CTP:phosphoethanolamine cytidylyltransferase (Pcyt2). *Biochem Cell Biol*. 2007;85:283-300.
52. Vance JE, Tasseva G. Formation and function of phosphatidylserine and phosphatidylethanolamine in mammalian cells. *Biochim Biophys Acta*. 2013;1831:543-554.
53. Tuladhar R, Yarravarapu N, Ma Y, et al. Stereoselective fatty acylation is essential for the release of lipidated WNT proteins from the acyltransferase porcupine (PORCN). *J Biol Chem*. 2019;294:6273-6282.
54. Nile AH, Hannoush RN. Fatty acylation of Wnt proteins. *Nat Chem Biol*. 2016;12:60-69.
55. Kalgutkar AS, Hatch HL, Kosea F, et al. Preclinical pharmacokinetics and metabolism of 6-(4-[2,5-difluorophenyl]oxazol-5-yl)-3-isopropyl-[1,2,4]-triazolo[4,3-a]pyridine, a novel and selective p38alpha inhibitor: identification of an active metabolite in preclinical species and human liver microsomes. *Biopharm Drug Dispos*. 2006;27:371-386.
56. Bikkavilli RK, Feigin ME, Malbon CC. p38 mitogen-activated protein kinase regulates canonical Wnt-beta-catenin signaling by inactivation of GSK3beta. *J Cell Sci*. 2008;121:3598-3607.
57. Hou X, Tan Y, Li M, Dey SK, Das SK. Canonical Wnt signaling is critical to estrogen-mediated uterine growth. *Mol Endocrinol*. 2004;18:3035-3049.
58. Shi B, Liang J, Yang X, et al. Integration of estrogen and Wnt signaling circuits by the polycomb group protein EZH2 in breast cancer cells. *Mol Cell Biol*. 2007;27:5105-5119.
59. Skah S, Uchuya-Castillo J, Sirakov M, Plateroti M. The thyroid hormone nuclear receptors and the Wnt/beta-catenin pathway: an intriguing liaison. *Dev Biol*. 2017;422:71-82.
60. Zhou H, Mak W, Kalak R, et al. Glucocorticoid-dependent Wnt signaling by mature osteoblasts is a key regulator of cranial skeletal development in mice. *Development*. 2009;136:427-436.
61. Ohnaka K, Tanabe M, Kawate H, Nawata H, Takayanagi R. Glucocorticoid suppresses the canonical Wnt signal in cultured human osteoblasts. *Biochem Biophys Res Commun*. 2005;329:177-181.
62. Crinnion WJ. The CDC fourth national report on human exposure to environmental chemicals: what it tells us about our toxic burden and how it assist environmental medicine physicians. *Altern Med Rev*. 2010;15:101-109.
63. TPMC. *Report on Carcinogens Background Document for Diethanolamine*. NIEHS, National Toxicology Program N01ES85421; 2002.
64. Fiume MM, Heldreth B, Bergfeld WF, et al. Safety assessment of Diethanolamine and its salts as used in cosmetics. *Int J Toxicol*. 2017;36:89S-110S.
65. The Personal Care Products Council. *International Cosmetic Ingredient Dictionary and Handbook*. 13th edition. The Personal Care Products Council; 2010.
66. Grosse Y, Baan R, Secretan-Lauby B, et al. Carcinogenicity of chemicals in industrial and consumer products, food contaminants and flavourings, and water chlorination byproducts. *Lancet Oncol*. 2011;12:328-329.
67. National Toxicology Program. NTP Toxicology and carcinogenesis studies of oleic acid Diethanolamine condensate (CAS no. 93-83-4) in F344/N rats and B6C3F1 mice (dermal studies). *Natl Toxicol Program Tech Rep Ser*. 1999;481:1-198.
68. Mathews JM, Garner CE, Matthews HB. Metabolism, bioaccumulation, and incorporation of diethanolamine into phospholipids. *Chem Res Toxicol*. 1995;8:625-633.
69. Niculescu MD, Wu R, Guo Z, da Costa KA, Zeisel SH. Diethanolamine alters proliferation and choline metabolism in mouse neural precursor cells. *Toxicol Sci*. 2007;96:321-326.
70. Craciunescu CN, Wu R, Zeisel SH. Diethanolamine alters neurogenesis and induces apoptosis in fetal mouse hippocampus. *FASEB J*. 2006;20:1635-1640.
71. Craciunescu CN, Niculescu MD, Guo Z, Johnson AR, Fischer L, Zeisel SH. Dose response effects of dermally applied diethanolamine on neurogenesis in fetal mouse hippocampus and potential exposure of humans. *Toxicol Sci*. 2009;107:220-226.
72. Lehman-McKeeman LD, Gamsky EA, Hicks SM, Vassallo JD, Mar MH, Zeisel SH. Diethanolamine induces hepatic choline deficiency in mice. *Toxicol Sci*. 2002;67:38-45.
73. Guo X, Wang XF. Signaling cross-talk between TGF-beta/BMP and other pathways. *Cell Res*. 2009;19:71-88.
74. Sanders LM, Zeisel SH. Choline: dietary requirements and role in brain development. *Nutr Today*. 2007;42:181-186.
75. Mehedint MG, Niculescu MD, Craciunescu CN, Zeisel SH. Choline deficiency alters global histone methylation and

epigenetic marking at the Re1 site of the calbindin 1 gene. *FASEB J*. 2010;24:184-195.
76. Niculescu MD, Craciunescu CN, Zeisel SH. Dietary choline deficiency alters global and gene-specific DNA methylation in the developing hippocampus of mouse fetal brains. *FASEB J*. 2006;20:43-49.
77. Williams AJ, Grulke CM, Edwards J, et al. The CompTox chemistry dashboard: a community data resource for environmental chemistry. *J Chem*. 2017;9:61.
78. Sharma A, Mir R, Galande S. Epigenetic regulation of the Wnt/beta-catenin signaling pathway in cancer. *Front Genet*. 2021;12:681053.
79. Obeid R. The metabolic burden of methyl donor deficiency with focus on the betaine homocysteine methyltransferase pathway. *Nutrients*. 2013;5:3481-3495.
80. Bachman AN, Kamendulis LM, Goodman JI. Diethanolamine and phenobarbital produce an altered pattern of methylation in GC-rich regions of DNA in B6C3F1 mouse hepatocytes similar to that resulting from choline deficiency. *Toxicol Sci*. 2006;90:317-325.
81. Hayashi SM, Ton TV, Hong HH, et al. Genetic alterations in the Catnb gene but not the H-ras gene in hepatocellular neoplasms and hepatoblastomas of B6C3F(1) mice following exposure to diethanolamine for 2 years. *Chem Biol Interact*. 2003;146:251-261.
82. Commission" E. CosIng Database . Annex II. List of substances which must not form part of the composition of cosmetic products. Secondary alkyl- and alkanolamines and their salts, including diethanolamine; 2001.
83. Canada. *Cosmetic Ingredient Hotlist*; 2019. Accessed March 3, 2022. https://www.canada.ca/en/health-canada/services/consumer-product-safety/cosmetics/cosmetic-ingredient-hotlist-prohibited-restricted-ingredients/hotlist.html#t1d

SUPPORTING INFORMATION

Additional supporting information may be found in the online version of the article at the publisher's website.

How to cite this article: Wolter JM, Jimenez JA, Stein JL, Zylka MJ. ToxCast chemical library Wnt screen identifies diethanolamine as an activator of neural progenitor proliferation. *FASEB BioAdvances*. 2022;4:441–453. doi:10.1096/fba.2021-00163